

IDENTIFICATION OF SPINNING DUST IN H α -CORRELATED MICROWAVE EMISSION

GREGORY DOBLER^{1,2} & DOUGLAS P. FINKBEINER^{1,3}

Draft version November 18, 2018

ABSTRACT

CMB experiments commonly use maps of H α intensity as a spatial template for Galactic free-free emission, assuming a power law $I_\nu \propto \nu^{-0.15}$ for the spectrum. Any departure from the assumed free-free spectrum could have a detrimental effect on determination of the primary CMB anisotropy. We show that the H α -correlated emission spectrum in the diffuse WIM is *not* the expected free-free spectrum at WMAP frequencies. Instead, there is a broad bump in the spectrum at ~ 50 GHz which is consistent with emission from spinning dust grains. Spectra from both the full sky and smaller regions of interest are well fit by a superposition of a free-free and “warm ionized medium” Draine & Lazarian (1998) spinning dust model, shifted in frequency. The spinning dust emission is ~ 5 times weaker than the free-free component at 50 GHz, with the null hypothesis that the H α -correlated spectrum is pure free-free, ruled out at $\geq 8\sigma$ in all regions and $> 100\sigma$ for the full sky fit.

Subject headings: diffuse radiation — dust, extinction — ISM: clouds — radiation mechanisms: non-thermal — radio continuum: ISM

1. INTRODUCTION

During the course of measuring the cosmic microwave background (CMB) anisotropy, the *Wilkinson Microwave Anisotropy Probe* (WMAP) has produced the most detailed and sensitive maps of interstellar medium (ISM) emission between 20 and 100 GHz taken to date. The quality of the data has profoundly influenced our understanding of the four main ISM continuum emission mechanisms in this frequency range (Bennett et al. 2003; Finkbeiner 2003; Hinshaw et al. 2007; Dobler & Finkbeiner 2007). At the highest WMAP frequencies, the Galaxy is dominated by thermal dust emission, traced by far IR maps (Finkbeiner et al. 1999). At lower frequencies, synchrotron radiation from supernova shock accelerated electrons spiraling in the Galactic magnetic field makes up the majority of the emission. In the inner Galaxy, the synchrotron emission is brighter relative to low-frequency maps, and has a harder spectrum.⁴ Next, free-free emission from unbound electrons interacting with ions in $\sim 10^4$ K ionized gas has a harder spectrum than synchrotron, and is detectable in all bands. Finally, there is a bump in the spectrum of dust-correlated emission at ~ 20 GHz, sometimes called “Foreground X” (de Oliveira-Costa et al. 2002). Over the last decade, it has been recognized that this could be electric dipole emission from rapidly rotating dust grains (“spinning dust”; Draine & Lazarian 1998b).

1.1. *Foreground X: spinning dust?*

Spinning dust is the electric dipole emission from the smallest dust grains which have a non-zero electric dipole moment and are spun up by several different interactions with the interstellar medium (e.g., ion collisions, the interstellar radiation field, etc.; see Draine & Lazarian 1998b). Spinning dust was considered as a potential source of radio and microwave emission in other contexts (Erickson 1957; Ferrara & Dettmar 1994). Because the model depends on the grain size distribution, ionization fraction, electric dipole moments, etc., the peak frequency can be anywhere from 10 – 50 GHz, but is usually in the 20 – 40 GHz range. This dependence of the spectrum on the ISM parameters has made spinning dust difficult to definitively identify, but may provide the qualitative behaviors necessary to make a fool-proof detection.

In the COBE/DMR data, Kogut et al. (1996) found that the dust-correlated emission does not simply fall off monotonically with decreasing frequency as would be expected for a thermal dust tail, but instead was greater at 31 GHz than at 53 GHz. This behavior was confirmed by the Saskatoon CMB experiment (de Oliveira-Costa et al. 1997), the 14.5 and 32 GHz OVRO data (Leitch et al. 1997), the Cottingham & Boughn 19.2 GHz survey (de Oliveira-Costa et al. 1998), the Tenerife 10 & 15 GHz survey (de Oliveira-Costa et al. 1999), and the QMAP 30 GHz data (de Oliveira-Costa et al. 2000). A small survey of dust clouds with the Green Bank 42m telescope at 5, 8, & 10 GHz (Finkbeiner et al. 2002) revealed two candidates for spinning dust clouds: L1622, later confirmed (Finkbeiner 2004); and LPH 201.663+1.643, which turned out to be incorrect (Dickinson et al. 2006).

Given this evidence, it was already clear prior to the WMAP data release in early 2003, that there was some non-standard emission mechanism, but it was unclear whether this mechanism was spinning dust (Draine & Lazarian 1998b) or some other process.

WMAP (Bennett et al. 2003) found that the dust-correlated emission falls from 94 to 61 GHz and then rises steadily to 23 GHz. The fact that synchrotron typi-

¹ Institute for Theory and Computation, Harvard-Smithsonian Center for Astrophysics, 60 Garden Street, MS-51, Cambridge, MA 02138 USA

² gdobler@cfa.harvard.edu

³ dfinkbeiner@cfa.harvard.edu

⁴ Finkbeiner (2004) has previously interpreted this as a separate component, the synchrotron “haze”, but this interpretation is controversial (Finkbeiner 2004; Dobler & Finkbeiner 2007). This haze component is spatially orthogonal to the other templates by construction, and though we include it in our fits below, its existence has negligible effect on the H α -correlated spectrum.

cally dominates at lower frequencies led Bennett et al. (2003) to interpret the low frequency rise as “dust-correlated synchrotron”. The reasoning was that because dusty regions correlate with regions of star formation activity, electrons in the vicinity could be accelerated by supernova shocks leading to synchrotron emission. Finkbeiner (2004) pointed out that WMAP is also consistent with Draine & Lazarian (1998b) if their model could be shifted down in frequency a bit.

Because the WMAP frequency coverage (23 – 94 GHz) coincides with the range where the spinning dust and synchrotron spectra are similar, data at lower frequencies, where the spectra diverge, have been used to test the dust-correlated synchrotron hypothesis. The WMAP “synchrotron” template has a much weaker cross-correlation at 10 – 15 GHz than expected for actual synchrotron (de Oliveira-Costa et al. 2004). Also, 8 & 14 GHz data from the Green Bank Galactic Plane Survey (Langston et al. 2000) show a rising spectrum consistent with spinning dust but not synchrotron (Finkbeiner, Langston, & Minter 2004) and implying that the majority of dust-correlated emission at 23 GHz is Foreground X. Comparing the Cottingham & Boughn survey to WMAP also shows a rise from 19 to 23 GHz (Boughn & Pober 2007). The polarization properties (Page et al. 2007; Hinshaw et al. 2007) in the 3-yr WMAP data also favor the spinning dust hypothesis.

In spite of all this evidence, there are weaknesses in each of these arguments. Some use only low-latitude data and may not apply to the diffuse ISM (Finkbeiner, Langston, & Minter 2004). Others apply to only one cloud (Finkbeiner et al. 2002), have poor signal to noise (de Oliveira-Costa et al. 2004), or a short lever arm in frequency (Boughn & Pober 2007). However, taken together, they are very strong evidence against the dust-correlated synchrotron hypothesis, but they are not specifically evidence *for* spinning dust. Other mechanisms such as magnetic dipole dust emission, caused by the thermal fluctuation of the magnetization in the dust grains (Draine & Lazarian 1999), could conceivably explain all these results. This ambiguity motivated our search for further clues in the WMAP 3-yr data.

1.2. WMAP Multilinear Regression

In Dobler & Finkbeiner (2007, hereafter, DF07) we describe our method for determining the spectral shape of each of the four primary WMAP foreground components: free-free, dust, soft synchrotron, and hard synchrotron (termed the “haze” by Finkbeiner 2004) emission. We model the WMAP data as a linear combination of the CMB and the 4 foregrounds, each described by a specific spatial template. For free-free emission we use the H α map described in §2.1, for dust (thermal and spinning) emission we use the Schlegel et al. (1998) dust map evaluated at 94 GHz by Finkbeiner et al. (1999), for soft synchrotron we use the Haslam et al. (1982) 408 MHz map, and for the haze we use a simple $1/r$ template where r is the distance from the Galactic center. The individual WMAP bands were completely decoupled in our fit, and we assumed *nothing* about the spectrum of each foreground, only that its morphology was traced by the template in all bands. We performed our fits over both the (nearly) full sky and also on smaller regions of interest. Point sources and regions where

dust extinction makes the H α map unreliable (where $A(\text{H}\alpha) = 2.65 E(B-V) > 1$ mag) were masked out from the fits.

We showed that the spectrum of H α -correlated emission is *not* the usual free-free spectrum. Rather, there is a bump around $\nu \sim 50$ GHz. In §2.3 we explain why the H α map should actually trace spinning dust excited by collisions with ions. In §3 we present H α -correlated emission spectra for both the (nearly) full sky as well as smaller regions of interest and show that, indeed, the spectra are well characterized as a superposition of free-free and spinning dust type spectra. We summarize this work and discuss implications for future observations in §4.

2. EMISSION MEASURE AS A TRACER OF SPINNING DUST

In this section we argue that in fully ionized environments, the emissivity density (j_ν) of spinning dust emission is proportional to dust density times some excitation function related to the ion density. The emission comes from the very smallest grains, which are spun up by a collision with an ion and spin down as they radiate. In the limit where the spin down time is small compared to the time between collisions, the rotation is episodic and the emissivity also scales linearly with the ion number density. In §2.2, we assume the episodic limit in order to build some intuition about how WIM-correlated spinning dust might behave.

2.1. Free-free emission measure

The map assembled by Finkbeiner (2003) from the VTSS (Dennison et al. 1998), SHASSA (Gaustad et al. 2001), and WHAM (Haffner et al. 2003) surveys, traces the H α recombination line emission from hot interstellar gas. At WMAP frequencies, this H α map⁵ is used to estimate the thermal bremsstrahlung, or free-free emission, resulting from the interaction of the electrons and protons from ionized hydrogen (Bennett et al. 2003; Finkbeiner 2004; Hinshaw et al. 2007). The H α map is corrected for dust absorption using the prescription given by Finkbeiner (2003; but see Dickinson et al. 2003 for an alternative). In this frequency range the free-free specific intensity I_ν (in Jy/sr) is often approximated as a power law,

$$I_\nu \propto \nu^\alpha, \quad (1)$$

with $\alpha \approx -0.15$. Although this is a good approximation, in our analysis we use the expression given by Spitzer (1978) for the free-free spectrum.

Recombination line emission is a two particle process (involving the capture of free electrons by a proton nucleus) and so the emissivity is proportional to $n_e n_i$, which for fully ionized H is simply the square of the number density of gas particles, $j_{\text{H}\alpha} \propto n^2$. Therefore, the H α intensity corresponds to an *emission measure* (EM) defined as $E_m \equiv \int n^2 dl$ where the integral is taken along the line of sight. The H α intensity is usually measured in Rayleighs (1 R $\equiv 10^6/4\pi$ photons s⁻¹ cm⁻² sr⁻¹) with an EM of 1 cm⁻⁶pc ≈ 0.6 R for gas at ~ 8000 K.

⁵ available at <http://www.skymaps.info>

2.2. Spinning dust emission measure

Draine & Lazarian (1998b, hereafter, DL98) present a model for spinning dust emission in which tiny dust grains with non-negligible electric dipole moment are spun up by ion collisions; polycyclic aromatic hydrocarbons (PAHs) generally have a non-zero dipole, because perfect symmetry is rare in large molecules. DL98 estimated the astronomical value of this parameter (actually the electric dipole moment per root mass) from measured electric dipole moments for dozens of known PAH molecules. In the limit where ion interactions provide the dominant spin-up mechanism (see DL98 for details) and assuming full ionization, constant gas/dust ratio, and the same grain size distribution everywhere, the resulting *total* spinning dust emission is $I \equiv \int I_\nu d\nu \propto \int n_i n_d dl \propto \int n_i^2$. With the additional assumption that the emission is episodic, the spectrum of the emission does not vary with n_i , but the amplitude does. That is, the spinning dust emission should look like an EM, and be traced by H α . This approximation is relevant where the collisional excitation is primarily due to ions (at least for the smallest grains), e.g. for the “warm ionized medium” (WIM) parameters used by DL98.

The WIM-correlated emission claimed here augments the “usual” spinning dust emission in the “cold neutral medium” (CNM) which has a temperature $T_{\text{CNM}} \sim 100$ K and is traced by the Schlegel et al. (1998) dust map evaluated at 94 GHz by Finkbeiner et al. (1999) (FSD99).

2.3. Estimating the specific intensity

For a spherical dust grain of size a , rotating with angular frequency ω , and with a dipole moment p_0 , the rotational energy is,

$$E = \frac{1}{2} I \omega^2 = \frac{1}{5} m a^2 \omega^2, \quad (2)$$

where m is the grain mass. The energy loss rate is the total power emitted by the grain,

$$\dot{E} = \frac{1}{12\pi} \frac{\mu_0}{c} p_0^2 \omega^4 \quad (3)$$

and the spin down time is,

$$\tau_s \equiv E/\dot{E} \propto a^2 p_0^{-2} \omega^{-2}. \quad (4)$$

The time between collisions is just,

$$\tau_c \sim \lambda/v \propto a^{-2} n_H^{-1} \quad (5)$$

where v is the thermal velocity of the ion and $\lambda = (\pi a^2 n_H)^{-1}$ is the mean free path.

In the limit where the spin down time is much *smaller* than the time between collisions ($r \equiv \tau_s/\tau_c \ll 1$), the excitation is episodic. For the WIM parameters in DL98, this ratio is in fact ~ 1 ; however, we point out that

$$r = \tau_s/\tau_c \propto a^4 n_H p_0^{-2} \omega^{-2} \quad (6)$$

so that very small changes to the grain size distribution can substantially affect the spin down time compared to the time between collisions. In fact, if each ion collision imparts equal energy, then from Equation 2, $\omega \propto a^{-2}$. Since $p_0 \propto N^{1/2} \propto a^{3/2}$ (see DL98) then in this case, $1/r$ diverges as a^{-5} . The bottom line is that the episodic

approximation is sensitively dependent on the ion density, the dipole moment, and *especially* the grain size distribution. For the purposes of estimating a specific intensity, we will now assume the episodic approximation with the caveat that it may break down in dense environments, (e.g., HII regions. In fact, Scaife et al. 2007, find no evidence for spinning dust at 14.2 and 17.9 GHz in 16 Galactic HII regions) or for very small dipole moments. We emphasize that this does not affect the fact the *total intensity* I should be proportional to $\int n_d n_H dl$ so that spinning dust emission should be traced by an EM map.

Draine & Lazarian evaluate j_ν/n_H for parameters representative of various interstellar environments. In the limit that j_ν/n_H is a constant with n_H , then it equals $I_\nu/N(H)$. However, in our case it is not. As a reference model, we take the DL98 WIM model evaluated for $n_H = 0.1 \text{ cm}^{-3}$ which peaks near 25 GHz with a peak emissivity⁶ of $j_{p,\text{ref}}/n_H = 5 \times 10^{-21} \text{ kJy sr}^{-1} \text{ cm}^2$ or $j_{p,\text{ref}} = 5 \times 10^{-22} \text{ kJy sr}^{-1} \text{ cm}^{-1}$. Multiplying the dependence on dust and gas density we have⁷

$$j_p = j_{p,\text{ref}} \left(\frac{n_H}{n_{H,\text{ref}}} \right) \left(\frac{n_d}{n_{d,\text{ref}}} \right) \quad (7)$$

where $n_{H,\text{ref}}$ and $n_{d,\text{ref}}$ are the density of H and small dust grains, respectively, used in the reference model. For full ionization of H ($n_H = n_i$) and constant gas/dust ratio ($n_H/n_{H,\text{ref}} = n_d/n_{d,\text{ref}}$) we have

$$j_p = j_{p,\text{ref}} \left(\frac{n_H}{0.1 \text{ cm}^{-3}} \right)^2 \quad (8)$$

$$= 5 \times 10^{-20} n_H^2 \text{ kJy sr}^{-1} \text{ cm}^5 \quad (9)$$

$$= 0.15 n_H^2 \text{ kJy sr}^{-1} \text{ cm}^6 \text{ pc}^{-1} \quad (10)$$

and the peak specific intensity is then

$$I_p = \int j_p dl = 0.15 \text{ kJy sr}^{-1} \left(\frac{E_m}{1 \text{ cm}^{-6} \text{ pc}} \right) \quad (11)$$

or

$$I_p/I_{\text{H}\alpha} = 0.09 \text{ kJy sr}^{-1} \text{ R}^{-1}, \quad (12)$$

where $I_{\text{H}\alpha}$ is measured in R. For comparison, the ratio of free-free to H α for a temperature of $T_e \sim 8000\text{K}$ at 41 GHz (WMAP Q-band) is $I_{41}/I_{\text{H}\alpha} \sim 0.15 \text{ kJy sr}^{-1} \text{ R}^{-1}$.

Although this is a rough estimate, it suggests that the intensity of the free-free emission at 41 GHz and the peak of the spinning dust emission should be of the same order of magnitude. Throughout this discussion we make the assumption that the DL98 WIM spectrum can be shifted by a factor of 2 in frequency. A more thorough analysis would require that the DL98 model be evaluated for some set of parameters (ion density, electric dipole moment per root mass, etc.) that give the actual spectrum observed. For our purposes this naive shift is adequate.

⁶ The units of the ordinate, j_ν/n_H , of Figs. 9-11 in DL98 is incorrectly labeled (Jy sr^{-1}) rather than ($\text{Jy cm}^2 \text{ sr}^{-1}$), an error propagated by Finkbeiner et al. (2002).

⁷ Again, the dependence on n_H in Equation 7 is only strictly correct in the episodic limit, though in reality the deviation is likely small.

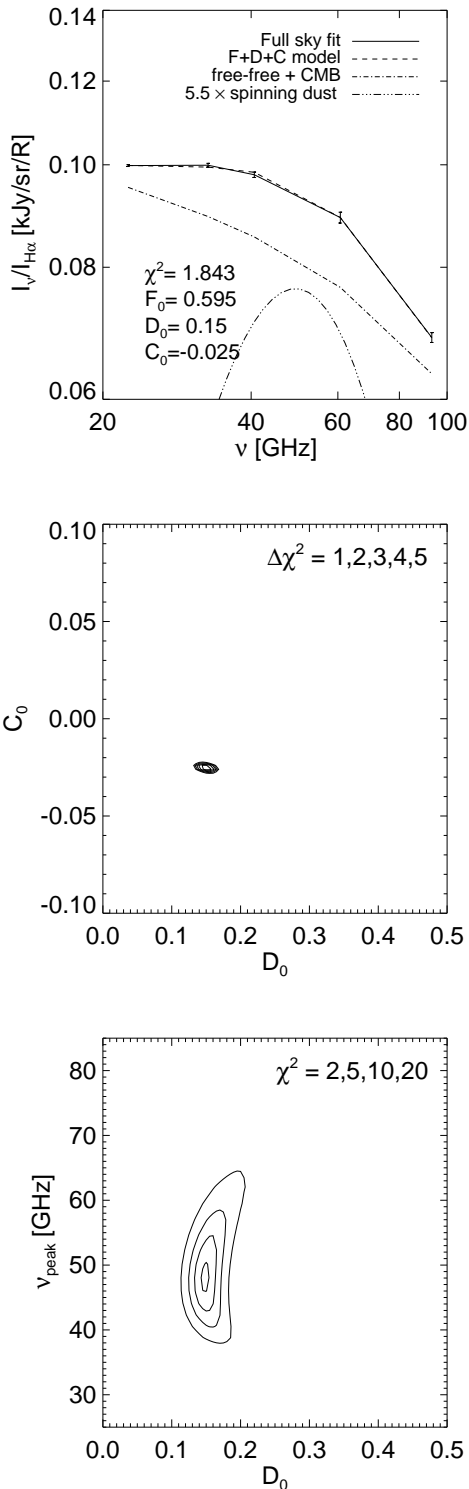


FIG. 1.— *Top panel:* The best $F+D+C$ (free-free plus spinning dust plus CMB) model fit to the $H\alpha$ -correlated emission over the full sky. The peak frequency is fixed to $\nu_{\text{peak}} = 50$ GHz. This two component plus CMB contamination model works surprisingly well with a spinning dust component that is 6.23 times weaker than the free-free (see Table 1). *Middle panel:* $\Delta\chi^2$ contours for the best fit free-free coefficient in the spinning dust/CMB plane. The null hypothesis that the $H\alpha$ -correlated emission can be well fit by only a $F+C$ model (i.e., $D_0 = 0$) is ruled out to very high confidence (335σ). *Bottom panel:* χ^2 contours in the spinning dust/ ν_{peak} plane. Though the peak frequency is not very well constrained, we can rule out $\nu_{\text{peak}} < 40$ GHz and $\nu_{\text{peak}} > 60$ GHz at $> 4\sigma$ confidence.

3. SPECTRUM OF $H\alpha$ -CORRELATED EMISSION

As noted above, in DF07 we showed that the spectrum of $H\alpha$ -correlated emission in the WMAP data has a bump around $\nu \sim 50$ GHz that we now argue is consistent with a spinning dust contamination of the familiar Equation 1 free-free spectrum. We also point out in DF07 that any measurement of a foreground spectrum is necessarily contaminated by a component which has the frequency dependence of the CMB due to imperfect foreground removal when constructing a CMB template.⁸ However, as we will show shortly, this contamination is incapable of producing the observed bump.

Figure 1 shows our full sky fit for $H\alpha$ -correlated emission. Our hypothesis is that this spectrum can be well fit by a linear combination of free-free, spinning dust, and CMB spectra. Thus, our model spectrum is

$$I_{\nu}^{\text{mod}} = F + D + C, \quad (13)$$

where

$$F = F_0 \left(\frac{\nu}{23 \text{ GHz}} \right)^{-0.15}, \quad (14)$$

$$D = D_0 \times (\text{DL98 WIM model with } \nu_p = 50 \text{ GHz}), \quad (15)$$

and

$$C = C_0 \left(\frac{\nu}{23 \text{ GHz}} \right)^2. \quad (16)$$

We minimize $\chi^2 = \sum_i (I_{\nu_i}^{\text{mod}} - I_{\nu_i})^2 / \sigma_i^2$ over the parameters F_0 , D_0 , and C_0 which are scaled to be of order unity. Here σ_i are the formal errors in band i of the spectrum from our DF07 template fit, and we have one degree of freedom.

As shown in Figure 1, the spectral model in Equation 13 fits the data astonishingly well. The free-free and spinning dust amplitudes are comparable while the contamination from the CMB is minimal. The very low value of $\chi^2 = 1.84$ reflects the quality of the fit. Figure 1 also shows $\Delta\chi^2 = 1, 2, 3, 4,$ and 5 contours in the D_0 - C_0 plane minimizing χ^2 over F_0 at each point, and holding ν_p fixed at 50 GHz. The null hypothesis that only a free-free plus CMB spectrum (i.e., $D_0 = 0$) fit the data is ruled out to a very high significance. Thus, either free-free emission does not follow Equation 1, or the $H\alpha$ map is tracing an additional emission component. This other emission component seems to be well fit by a shifted WIM spinning dust spectrum.

Lastly, the χ^2 contours in the D_0 - ν_{peak} plane in the bottom panel of Figure 1 indicate that, although the peak frequency of the spinning dust is not very well constrained, values of $\sim 45 - 55$ GHz are consistent with the data. Peak frequencies less than 40 GHz and greater than 60 GHz are ruled out at 4σ .

The next step is to consider smaller individual regions of the sky to show that the signal persists. Figures 2 and 3 show fits for four different regions of the Gum Nebula, the north central Galactic sky (including the Ophiuchus complex), and a region near the Orion Nebula (see Table 1 and Figure 4 for details). Though the fits are significantly noisier as a result of the smaller number of pixels used, the bump in the $H\alpha$ -correlated emission remains

⁸ Throughout this paper, we will work with the results found using our CMB5 estimator for the CMB – see DF07 for details.

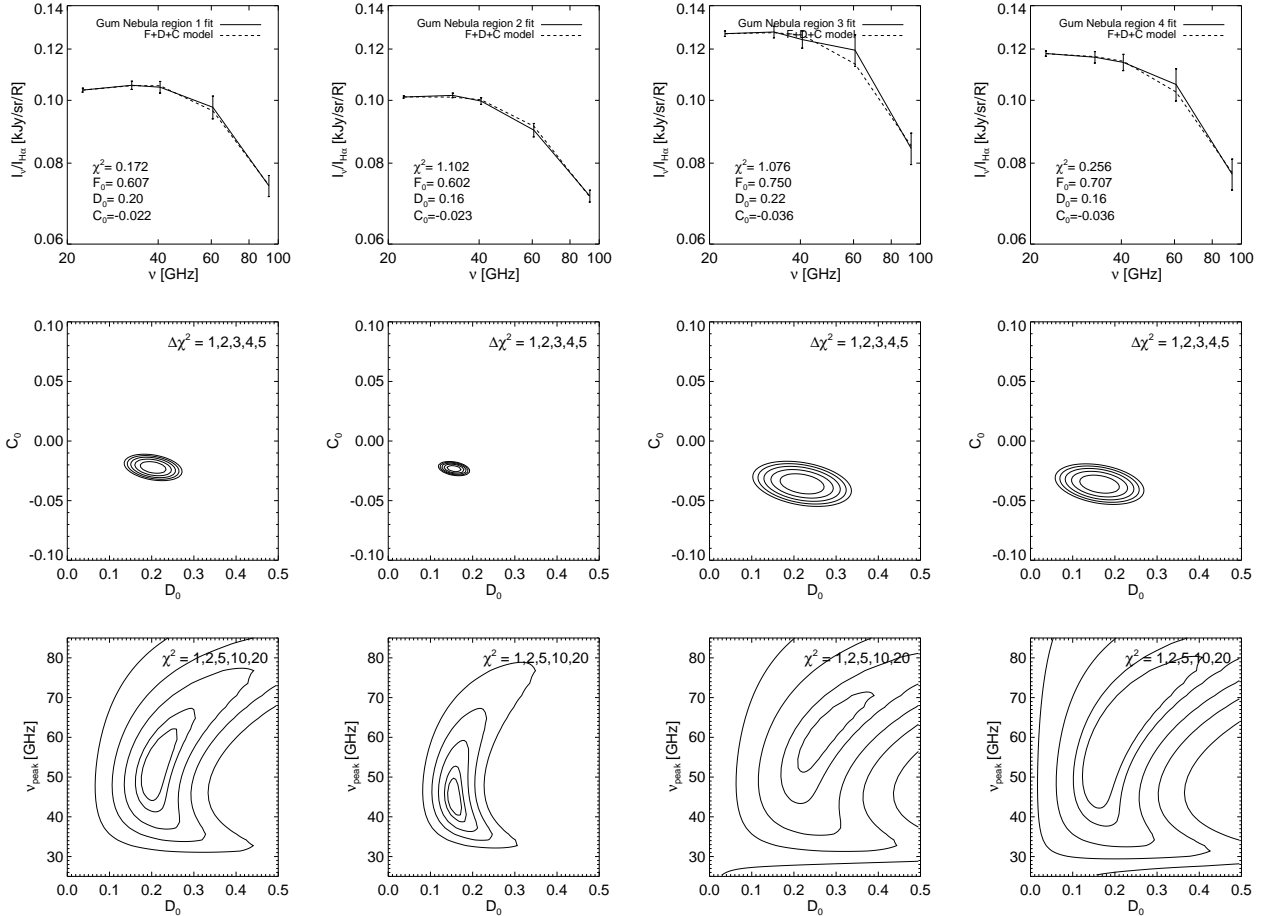


FIG. 2.— The same as Figure 1 except for the four regions of the Gum Nebula (see Table 1). Although the peak frequency is only loosely constrained, the $D_0 = 0$ null hypothesis is ruled out at $\geq 12\sigma$ in all regions.

TABLE 1

	Full sky	Gum Nebula				Ophiuchus	Orion
		1	2	3	4		
lrange	0:360	235:256	256:280	235:256	256:280	334:13	195:230
brange	-90:90	-30:0	-30:0	0:30	0:30	0:90	-35:0
χ^2	1.84	0.17	1.10	1.08	0.26	0.17	1.52
$\Delta\chi^2_{D=0}$	335.02	43.84	87.32	17.59	12.09	11.89	8.30
$I_F/I_D(\nu = \nu_{\text{peak}})$	6.23	4.70	6.07	5.38	6.80	4.75	12.22

NOTE.— Region definitions (in Galactic coordinates l and b) and results of the fits presented in Figures 1-3. The very low values of χ^2 reflect both the quality of the fits and the small number of constraints (number of degrees of freedom = 2). The $D_0 = 0$ null hypothesis is ruled out at $> 8\sigma$ in *all* regions, while the relative intensity of free-free to spinning dust emission at $\nu_{\text{peak}} = 50$ GHz is in the range 4.7-12.2.

in all regions, with the free-free amplitude roughly 4-7 times larger than the spinning dust. Furthermore, the case of no spinning dust $D_0 = 0$ is ruled out in *all* regions at $\geq 8\sigma$. Although the χ^2 contours in the D_0 - ν_{peak} plane offer a tantalizing hint that the peak frequency of the spinning dust is lower in the Orion Nebula region than the others, the present data are simply too noisy to make a statistically significant statement.

Lastly, we address the possibility that the bump in the H α -correlated emission represents a cross-correlation bias between the different templates used in DF07. That is to say, perhaps the H α spectrum is absorbing power

from other templates in the fit. Table 2 shows the correlation matrix, defined as

$$\Gamma_{i,j} = \frac{\langle T_i T_j \rangle}{\sqrt{\langle T_i^2 \rangle \langle T_j^2 \rangle}} \quad (17)$$

where $\Gamma_{i,j}$ is the correlation between the i th and j th template. The correlation between the templates is rather small. In particular, the dust map is the template which is most highly correlated with the H α map, and even then, the variance in the H α -correlated emission can be

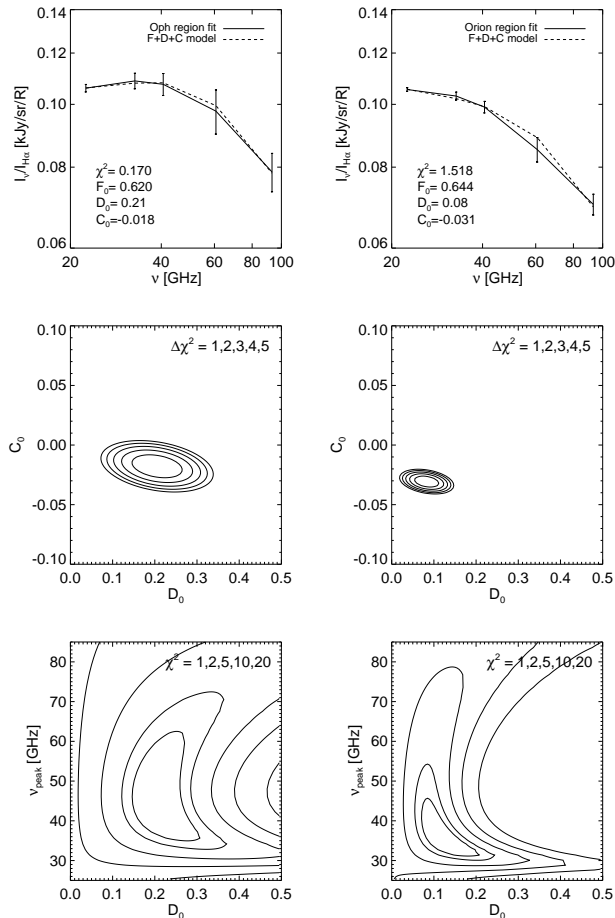


FIG. 3.— The same as Figure 1 except for a region which encloses the Ophiuchus Complex (left column) and one which is near the Orion Nebula (right column). See Table 1 for details.

TABLE 2

	H α	Dust	Haslam	Haze
H α	1.00	0.45	0.18	0.10
Dust	0.45	1.00	0.56	0.26
Haslam	0.18	0.56	1.00	0.58
Haze	0.10	0.26	0.58	1.00

NOTE. — The correlation matrix for the templates presented in Dobler & Finkbeiner (2007). These are the templates that were used in the multi-linear regression fit which revealed the bump in the H α -correlated emission presented in Figures 1-3.

at most $\Gamma_{\text{H}\alpha, \text{dust}}^2 = 20\%$ due to correlation with dust.

In fact, Figure 5 shows that the effects are much smaller. Here, the solid lines show the resultant spectra for all foreground components both with and without fitting the H α spectrum. In the latter case the H α emission was assumed to follow the free-free spectrum in Equation 1. The features of these spectra are discussed at length in DF07, but the important point is that the other foregrounds are not significantly affected when the H α spectrum is fixed. This is strong evidence that the emission mechanism causing the bump in the H α spec-

trum is highly correlated with the H α template.

4. DISCUSSION

In Dobler & Finkbeiner (2007) we identified a deviation from the classical free-free (thermal bremsstrahlung) spectrum in the H α -correlated emission of the 3-year WMAP data. In this paper we have argued that the spectral data are consistent with a superposition of free-free and spinning dust emission from a “warm ionized medium” (WIM; see Draine & Lazarian 1998b). Additionally, there is contamination by a component with the spectrum of the CMB due to chance morphological correlation between the CMB and the H α map (see Dobler & Finkbeiner 2007, for details).

Since the intensity of both free-free and WIM spinning dust emission scale proportionately with the number density squared (free-free emission is generated by the collision of free electrons with ions while the WIM spinning dust emission comes from collision of ions with tiny dust grains), both should be traced by an emission measure map like the H α map.

We have assumed throughout that the dust/gas ratio is constant and the grain size distribution is the same everywhere, so that $I \propto \int n_i n_d dl \propto \int n_i^2$.

We have studied both the (nearly) full sky and smaller independent regions of interest including the Gum Nebula, the Oph complex, and the Orion Nebula. For all regions, the H α -correlated emission is well fit by a linear combination of an $I_\nu \propto \nu^{-0.15}$ power law for free-free and a Draine & Lazarian (1998b) WIM spinning dust model shifted in frequency by a factor of 2 and with only a minimal adjustment in amplitude. Specifically, the spinning dust component is ~ 4 -7 times weaker than the free-free component.

The null hypothesis that a free-free only spectrum is consistent with the data is ruled out at $\geq 8\sigma$ confidence for all regions considered here, despite the substantial noise in the data. Furthermore, we have shown that the bump in the H α -correlated emission spectrum is *not* due to chance cross correlation between the H α map and the additional foreground templates presented in Dobler & Finkbeiner (2007), indicating that it is indeed correlated primarily with H α emission.

Finkbeiner et al. (2002) listed a number of criteria by which the existence of spinning dust could be established. Among them were that the peak frequency must shift as a function of the environment in a way at least qualitatively consistent with DL98. In this work we find in the WMAP data a WIM-correlated component with a peak frequency of 50 GHz, about a factor of two higher than the peak frequency of the spinning dust component that is spatially correlated with thermal dust emission (i.e. WNM or CNM spinning dust). That this frequency is higher is in accordance with the DL98 models, strongly supporting the spinning dust hypothesis. However, because the shift is larger than expected, a careful assessment of the situation requires that the reason for the size of the shift be determined. If, for example, the WIM dust has smaller grains, then a correlated measurement of $R_V \equiv A_V/E_{B-V}$ using e.g. background stars would complete the case for spinning dust.

In summary, there is clearly an additional foreground component correlated with H α emission and its spectral shape is consistent with spinning dust, though at a some-

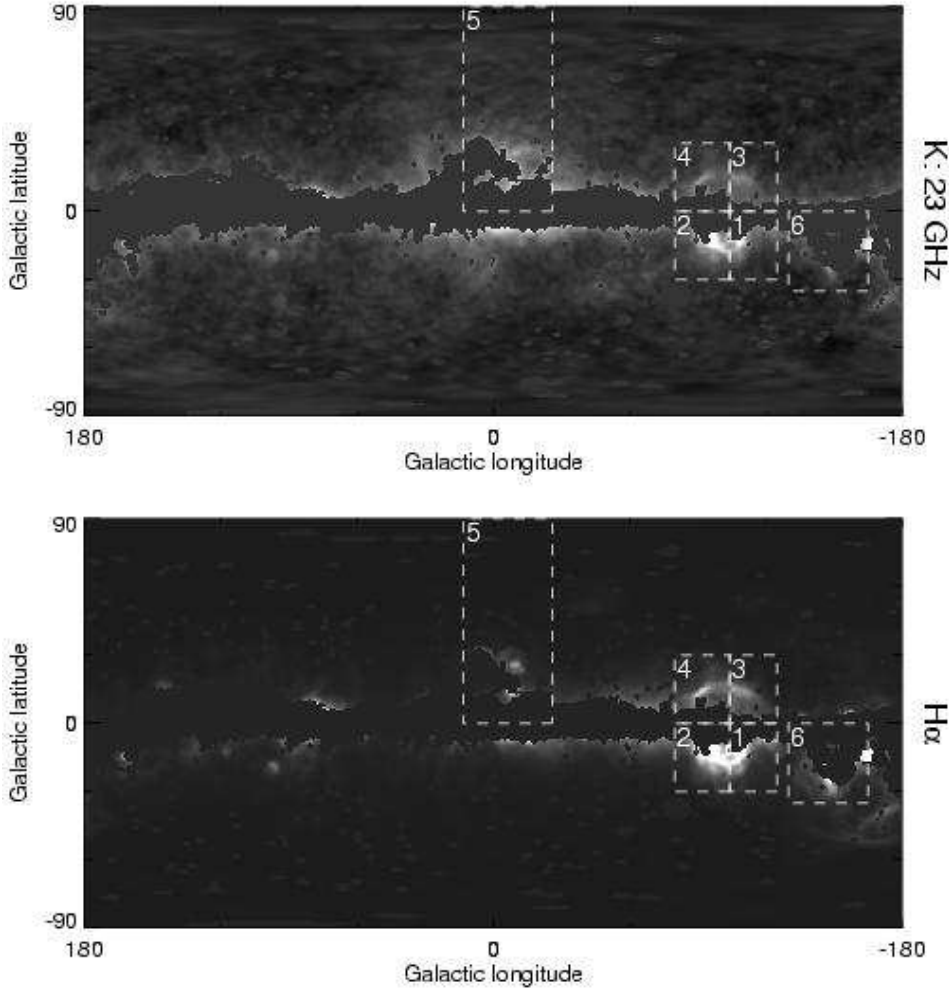


FIG. 4.— WMAP K band data (*top*) and the $H\alpha$ map (*bottom*) with our different fit regions shown as dotted boxes. In addition to the full sky fit, the regions are the Gum Nebula (1,2,3,4), the Ophiuchus complex (5), and the Orion Nebula (6). See Table 1 for details.

what higher frequency than expected. However, the increased sensitivity, frequency coverage, and finer spatial resolution of future missions like *Planck* may provide the necessary evidence.

We acknowledge helpful discussions with Bruce Draine, Gary Hinshaw, Joanna Dunkley, et al. Some of the

results in this paper were derived using HEALPix⁹ (Górski et al. 2005). This research made use of the NASA Astrophysics Data System (ADS) and the IDL Astronomy User’s Library at Goddard¹⁰. DPF and GD are supported in part by NASA LTSA grant NAG5-12972.

⁹ The HEALPix web page is <http://healpix.jpl.nasa.gov>

¹⁰ Available at <http://idlastro.gsfc.nasa.gov>

REFERENCES

- Bennett C.L. et al., 2003, *ApJS*, 148, 97
 Boughn S. P. & Pober J. C. 2007, *ApJ*, 661, 938
 Broderick A.E., Finkbeiner D.P., Afshordi N., & Dobler G., in preparation
 de Oliveira-Costa A., Kogut A., Devlin M.J., Netterfield C.B., Page L.A., & Wollack E.J., 1997, *ApJ*, 482, L17
 de Oliveira-Costa A., Tegmark M., Page L., & Boughn S., 1998, *ApJ*, 509, L9
 de Oliveira-Costa A. et al., 1999, *ApJ*, 527, L9
 de Oliveira-Costa A. et al., 2000, *ApJ*, 542, L5
 de Oliveira-Costa A. et al., 2002, *ApJ*, 567, 363
 de Oliveira-Costa A. et al., 2004, *ApJ*, 606, L89
 Dennison B., Simonetti J.H., & Topasna G., 1998, *Publ. Astron. Soc. Australia*, 15, 147
 Dickinson C., Davies R. D., & Davis R. J. 2003, *MNRAS*, 341, 369
 Dickinson C., Casassus S., Pineda J. L., Pearson T. J., Readhead A. C. S., & Davies, R. D. 2006, *ApJ*, 643, L111
 Dobler G. & Finkbeiner D.P., 2007, submitted to *ApJ*, arXiv:0712.1038
 Draine B.T. & Lazarian A., 1998a, *ApJ*, 494, L19
 Draine B.T. & Lazarian A., 1998b, *ApJ*, 508, 157
 Draine B.T. & Lazarian A., 1999, *ApJ*, 512, 740
 Erickson W. C. 1957, *ApJ*, 126, 480
 Ferrara A., & Dettmar R. -J. 1994, *ApJ*, 427, 155
 Finkbeiner D.P., Schlegel D.J., Frank, C., & Heiles C., 2002, *ApJ*, 566, 898
 Finkbeiner D.P., 2003, *ApJS*, 146, 407
 Finkbeiner D.P., 2004, *ApJ*, 614, 186
 Finkbeiner D.P., Davis M., & Schlegel D.J., 1999, *ApJ*, 524, 867
 Finkbeiner D. P., Langston G. I., & Minter A. H. 2004, *ApJ*, 617, 350

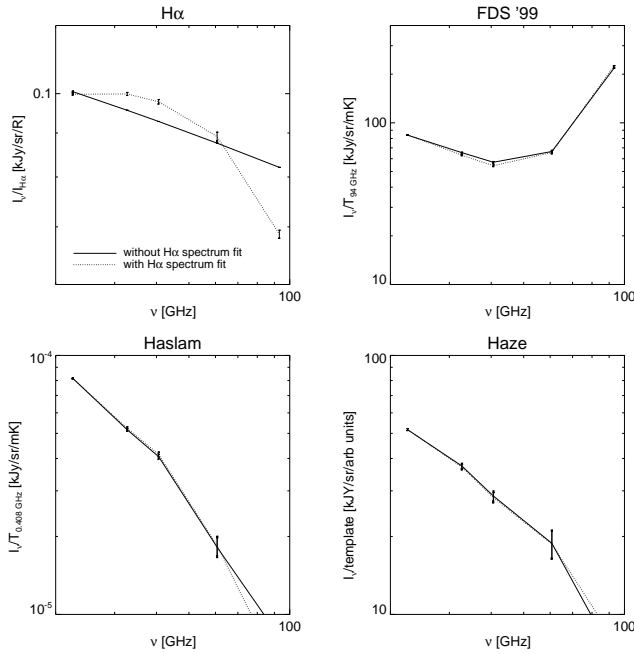


FIG. 5.— The intensity of the emission correlated with the four templates presented in Dobler & Finkbeiner (2007). The solid lines indicate fits for which the H α -correlated emission was constrained to follow a $I_{ff} \propto \nu^{-0.15}$ (see Equation 1) frequency dependence, while the dotted lines indicate that the H α -correlated spectrum was fit explicitly. Both the insensitivity of the inferred dust, Haslam, and haze -correlated spectra to fixing the H α spectrum as well as the relatively low correlation among the templates (Table 2) indicates that the spinning dust bump is indeed correlated primarily with H α emission.

- Gaustad J.E., McCullough P.R., Rosing W., & Van Buren D., 2001, PASP, 113, 1326
 Górski K.M. et al., 2005, ApJ, 622, 759
 Haslam C.G.T., Stoffel H., Salter C.J., & Wilson W.E., 1982, A&AS, 47, 1
 Haffner L.M., Reynolds R.J., Tuftes S.L., Madsen G.J., Jaehnig K.P., & Percival J.W., 2003, ApJS, 149, 405
 Hinshaw G. et al., 2007, ApJS, 170, 288
 Hooper D., Finkbeiner D.P., & Dobler G., 2007, arXiv:0705.3655
 Kogut A. et al., 1996, ApJ, 464, L5
 Langston, G., Minter, A., D'Addario, L., Eberhardt, K., Koski, K., & Zuber, J. 2000, AJ, 119, 2801
 Leitch, E. M., Readhead, A. C. S., Pearson, T. J., & Myers, S. T. 1997, ApJ, 486, L23
 Page, L. 2007
 Scaife A.M.M et al., 2007, arXiv:0711.3120
 Schlegel D.J., Finkbeiner D.P., & Davis M., 1998, ApJ, 500, 525
 Spergel D.N. et al., 2003, ApJS, 148, 175
 Spergel D.N. et al., 2007, ApJS, 170, 377
 Spitzer, L. 1978, *Physical Processes in the Interstellar Medium*, Wiley, New York